Deposition and spectral performance of an inhomogeneous broadband wide-angular antireflective coating

V. Janicki, D. Gäbler, S. Wilbrandt, R. Leitel, O. Stenzel, N. Kaiser, M. Lappschies, B. Görtz, D. Ristau, C. Rickers, and M. Vergöhl

Gradient index coatings and optical filters are a challenge for fabrication. In a round-robin experiment, basically the same hybrid antireflection coating for the visible spectral region, combining homogeneous refractive index layers of pure materials and linear gradient refractive index layers of material mixtures, has been deposited. The experiment involved three different deposition techniques: electron-beam evaporation, ion-beam sputtering, and radio frequency magnetron sputtering. The material combinations used by these techniques were Nb_2O_5/SiO_2, TiO_2/SiO_2, and Ta_2O_5/SiO_2, respectively. The spectral performances of samples coated on one side and on both sides have been compared to the corresponding theoretical spectra of the designed profile. Also, the reproducibility of results for each process is verified. Finally, it is shown that ion-beam sputtering gave the best results in terms of deviation from the theoretical performance and reproducibility.

OCIS codes: 310.1210, 310.1620, 310.1860.

1. Introduction

Multiple reflections between different surfaces in optical systems are undesirable because they contribute to a loss of intensity of transmitted light, a decreased contrast of the obtained image, and cause the appearance of ghost images. Therefore antireflective (AR) coatings are an important subject of thin-film optics. As a conclusion from the maximum principle,[1] the most efficient design for an AR coating for normal incidence will be obtained by using only two materials having the highest possible difference in refractive indices. In the case of wide-angular or omnidirectional AR coatings, this conclusion no longer holds, and it may be useful to introduce one or more additional materials or, finally, gradient index layers.

When this research was performed V. Janicki (janicki@irb.hr), D. Gäbler, S. Wilbrandt, R. Leitel, O. Stenzel, and N. Kaiser were at the Fraunhofer Institut für Angewandte Optik und Feinmechanik, Albert Einstein Strasse 7, 07745 Jena, Germany. V. Janicki is now with the Institut Ruđer Bošković, Bijenička 54, 10000 Zagreb, Croatia. M. Lappschies, B. Görtz, and D. Ristau are with the Laser Zentrum Hannover, Hollerithalle 8, 30419 Hannover, Germany. C. Rickers and M. Vergöhl are with Fraunhofer Institut für Schicht- und Oberflächentechnik, Bienroder Weg 54 E, 38108 Braunschweig, Germany.

Received 3 January 2006; revised 8 May 2006; accepted 9 June 2006; posted 14 June 2006 (Doc. ID 66897).

0003-6935/06/307851-07$15.00/0

The ideal AR coating for a given spectral and angular range would be a gradient refractive index structure of sufficient thickness having a refractive index varying smoothly from the value of the substrate, at the substrate side, to the value of the incident medium.[2–4] If the surrounding medium is air, the coating should terminate with a refractive index close to 1. It is possible to obtain such low values of refractive index by increasing the porosity of the film[5] or using the so-called moth's eye structures.[6] The drawback of these approaches is poor mechanical resistance and the difficulty cleaning such surfaces.

Besides sol–gel methods,[7,8] there are two more standard techniques for obtaining gradient layers with varying composition and refractive index in the growth direction. The first approach is based on changing the composition of ternary compounds during the growth of the layer by controlling the composition of the reactive gas.[9] The second technique involves coevaporation of two materials in which the ratio of particles of the two codeposited materials condensing at a substrate is varied.[10]

In this paper, deposition techniques and spectral performances of a hybrid AR coating for the visible spectral region are presented. In this context, the term "hybrid" describes a combination of linear gradient index layers (ramps) with layers of constant refractive index. Introducing an additional degree of freedom, i.e., the possibility of gradual transition from one value of refractive index to another, a simple

and feasible AR design has been obtained[11–13] and deposited.

2. Design

The desired spectral characteristics of the required AR coating for the BK7 glass substrate is defined by minimal reflectance R in the wavelength range 480–680 nm for incidence angles ranging from 0° to 50° and, additionally, equal s (R_s) and p (R_p) polarized reflectance at a 50° angle of incidence, respectively. Here $R = (R_s + R_p)/2$.

The hybrid design obtained[11] was refined to the available materials of each utilized deposition technique. For radio frequency magnetron sputtering (RFS), an additional, thicker design, having even better performance, has been prepared as well. To check the real benefits of this more complex coating, once when it is fabricated, its performance is compared to the sample with the simpler (thinner) coating.

The designs obtained are presented in Fig. 1 in conjunction with their corresponding reflectance values at 0° and 50° in Figs. 2(a) and 2(b), respectively. Some characteristics of the designs obtained for each applied deposition technique are presented in Table 1. The designs and their quality are almost the same, which can be seen from a comparison of the minimum (n_m) and maximum (n_M) refractive indices of the mixtures used in the designs and later in the depositions, total thickness, and deviation. The deviation was calculated according to

$$\delta_{\mathrm{TH}} = \sqrt{\frac{\sum_{i,j} [R_{i,\mathrm{TH}}(\lambda_j) - R_{i,\mathrm{TAR}}(\lambda_j)]^2}{N(N-1)}}, \qquad (1)$$

where R_{TH} and R_{TAR} are theoretical and target reflectance values at the given wavelength λ_j. The index i denotes average polarization for a 0° angle of incidence and s and p polarization for a 50° angle of incidence. The target values of reflectance, for a given

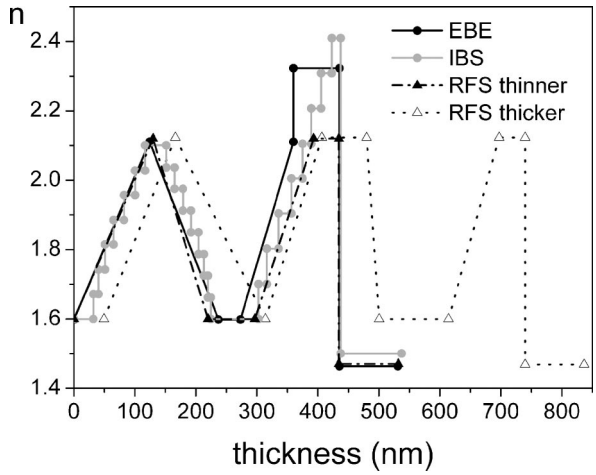

Fig. 1. Designs proposed for each deposition technique. For RFS there are two proposed designs, the thinner one and the thicker one, the latter has a lower deviation from the target, but is more demanding for deposition.

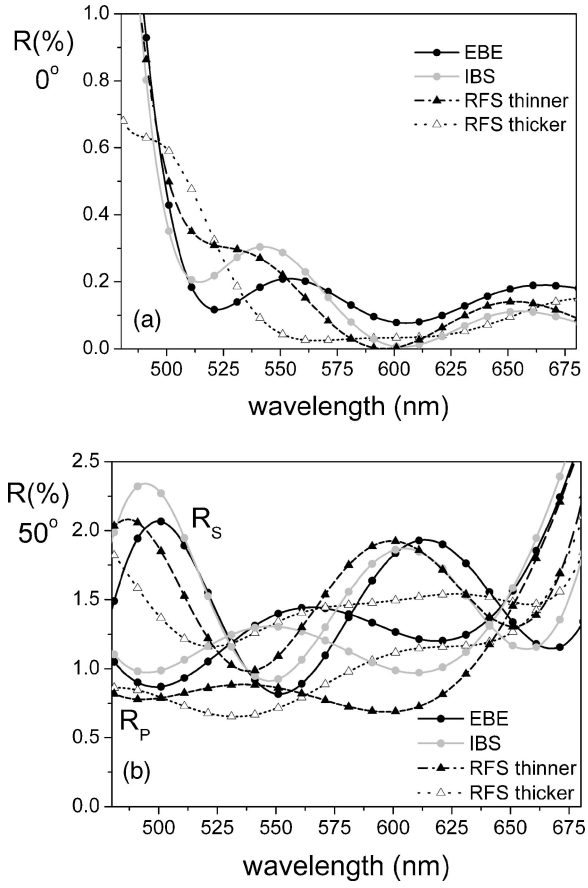

Fig. 2. Theoretical reflectance spectra of a glass surface (no backside reflection) coated with the designs presented in Fig. 1 for (a) angles of incidence of 0° and (b) as defined in specifications, 50°. One uncoated glass surface reflects 4% of light at 0° angle of incidence in the presented spectral range [see Fig. 3(a), for instance].

polarization and angle of incidence, were defined in the wavelength range 480–680 nm, and were each 1 nm. The parameter N denominates the total number of points where target values have been defined.

The intermediate refractive index at each point of the profile corresponds to the refractive index of a mixture of the two pure materials in appropriate concentrations. The intermediate indices are calculated according to the following mixture law:

$$n(\lambda) = \mu n_H(\lambda) + (1 - \mu) n_L(\lambda), \qquad (2)$$

where n_H and n_L stand for the refractive indices of high and low index pure materials, respectively. The coefficient μ is the volume fraction of the high index material in the mixture and can take values between 0 and 1. By using Eq. (2) the dispersion is included into the calculation of the spectral performance. Absorption is neglected because the absorption coefficient of the given materials is small in the required wavelength range, and the total thickness of the coating is low. Each gradient layer has been divided into eight homogeneous sublayers of equal thickness. This division has been shown to be a good approximation

Table 1. Refined Designs

Deposition Technique	Materials, Refractive Index at 570 nm	Minimum (n_m) and Maximum Refractive Index (n_M) at 570 nm	Total Thickness (nm)	Deviation from the Target (δ_{TH})
EBE	SiO_2 1.463	$n_m = 1.598$	531	0.0161
	Nb_2O_5 2.322	$n_M = 2.111$		
RFS Thinner	SiO_2 1.469	$n_m = 1.600$	532	0.0183
Thicker	Ta_2O_5 2.123	$n_M = 2.123$	837	0.0127
IBS	SiO_2 1.500	$n_m = 1.600$	537	0.0172
	TiO_2 2.409	$n_M = 2.308$		

of the inhomogeneous layer in order to compute the theoretical performance of the design by the matrix method.[14]

3. Experiment

A. Electron-Beam Evaporation

A Leybold Syrus Pro 1100 deposition system has been used previously with success for coevaporation of Nb_2O_5/SiO_2 mixture coatings and gradient index films.[15,16] The chamber was equipped with two electron beam guns and the advanced plasma source (APS).[17] The deposition of the materials (Nb_2O_5 and SiO_2) was performed in an atmosphere of argon as the working gas. Additionally, oxygen was employed as reactive gas to maintain the stoichiometry of the evaporated materials.

The refractive index changed due to the varying concentrations of the deposited materials in the layer. This was achieved by a continuous modification in deposition rates of the individual materials. The inhomogeneous profile in the fabricated coating was, therefore, a real continuous change of the layer properties and not a succession of thin homogeneous layers, i.e., quasi-inhomogeneous coating. The rate of deposition for each material was computer controlled and measured by two quartz crystal monitors, one for each material. The crystal monitors were shielded from each other to minimize their mutual cross talk. The deposition process is controlled by computer software enabling simultaneous automatic measurements and the acquisition of parameters (rates, pressures, and temperature) during the deposition.

The range of available feasible refractive indices by the deposition system is restricted to account for the fact that it was impossible to achieve stable and reproducible arbitrarily low deposition rates for the given materials. Therefore the initial design was refined with respect to the minimum rate of 0.2 nm/s and the maximum rate of 1.2 nm/s giving the range of refractive index constrained between 1.60 and 2.11 at a wavelength of 570 nm. The total rate of deposition during coevaporation was kept constant and set to the value of 1.4 nm/s. Therefore the deposition of the AR coating lasted approximately 9 min. To determine the refractive index and rate of deposition r at every moment of the film growth, it was necessary to perform the characterization of $n(\lambda)$ and calibration of rates for individual materials prior to the deposition of the coating. A thick single layer of each material has been fabricated for this purpose, varying r linearly and periodically between 0.2 and 1.2 nm/s during the deposition. After the characterization of n and rate of deposition tooling factors for quartz monitors were determined and thus calibration of r was performed.

B. Radio Frequency Magnetron Sputtering

The RFS experiments were performed by using a laboratory coater designed and constructed at the Institut für Schicht- und Oberflächetechnik for materials development. The chamber can be equipped with up to five 4 inch magnetron round sources (GENCOA, Limited) with three sources directed toward the substrate and allowing codeposition from up to three target materials. For the coating experiments, ceramic target materials were used (SiO_2 and Ta_2O_5) to avoid process instabilities due to coupling effects. The desired material composition was achieved by variation of the power ratio of the two sources and thus the individual deposition rates of each component of the mixture. During the processes a constant total power of 800 W as well as constant gas flows [Ar = 59 SCCM, O_2 = 4 SCCM (SCCM denotes cubic centimeters per minute at standard temperature and pressure), purities: Ar = 99.998 and O_2 = 99.995] were maintained. The O_2 gas flow was necessary for the realization of a stoichiometric Ta_2O_5 component of the mixture.

The calibration procedure used for the rates and refractive indices of the various material mixtures is comparable to the one described in Subsection 3.A. Single thick layers were realized and analyzed using spectral multiangle ellipsometry. The data acquired using this analysis, together with process parameters (mainly gas flows and power ratio), were then compiled into a material database. The software controller of the deposition plant can use this database to generate a deposition recipe. For the presented depositions no *in situ* monitoring of film properties or deposition rates was used.

Further improvements of the already excellent process stability could be achieved using *in situ* diagnostics of the growing film. The rates could theoretically be enhanced by increasing the total power as well as reactive gas flow depending on the material mixture. This seems appropriate since the deposition of stoichiometric SiO_2 is feasible from a ceramic target without the use of reactive gas flow. Furthermore, the

Table 2. Characteristics of the Deposition Techniques[a]

Deposition Technique	Rate of Deposition (nm/s)	Deposition Time (min)	Thickness Control	Optical Monitoring	Estimated Deviation in Thickness	Estimated Deviation in Refractive Index
EBE	1.4	9	Time	No	6%	0.6%
RFS	0.14	89 Thinner 114 Thicker	Time	No	1.5%	0.25%
IBS	0.035	260	Optical Thickness Determination	Yes	2%	0.2%

[a]Estimated deviations in thickness and in refractive indices correspond to mixture layers.

use of metallic target materials in combination with a controlled reactive process would dramatically increase rates. However, the control of such a coupled process is quite difficult and requires special measurement devices. Another potential benefit of using the magnetron-sputtering technique is the comparably easy feasibility of upscaling.

C. Ion Beam Sputtering

For ion-beam sputtering (IBS) the rebuilt Varian 3125 deposition chamber was equipped with a radio frequency ion source.[18] Argon ions were accelerated to energy values at approximately 1.2 keV for reactive sputtering from metallic targets. In this setup the target materials silicon and titanium were arranged side by side on the cooling body and were mounted on a linear translation stage.[19] Thus both materials could be sputtered simultaneously. The position of this target zone with respect to the ion beam defined the concentration of the oxide mixtures of SiO_2 and TiO_2, as the individual sputter maces superposed. The reactive process for film growth was operated at a pressure of 3×10^{-4} mbar. In this way an arbitrary refractive index from pure SiO_2 to pure TiO_2 could be realized with deposition rates between 0.06 and 0.02 nm/s and sufficient homogeneity on substrates with diameters up to 25 mm. A shutter was protecting the substrates when the target was preconditioned with the ion beam.

The implemented *in situ* broadband CCD monitoring system[20] recorded the calibrated transmittance

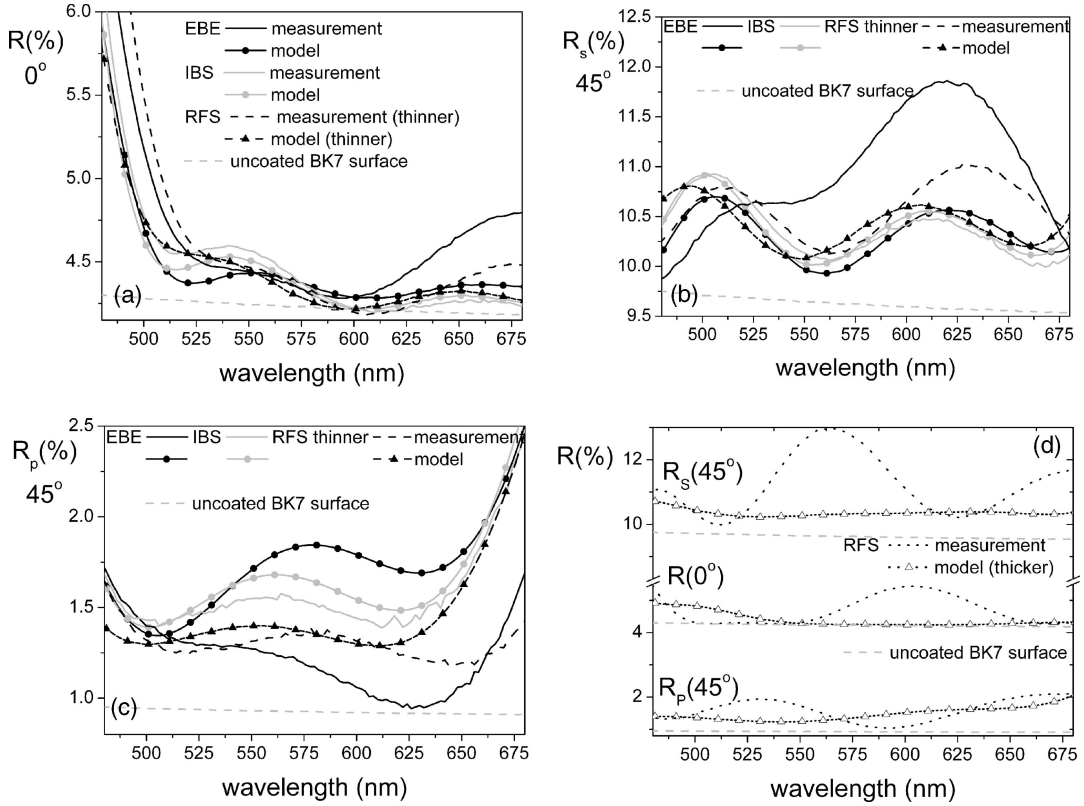

Fig. 3. Experimental and theoretical reflectance spectra of samples coated on one side. Spectra of the thinner coatings and designs are shown at (a) 0°, (b) *s* and (c) *p* polarization at 45° angle of incidence. Reflectance of one uncoated glass surface is also shown for comparison. (d) Corresponding spectra for the thicker RFS coating and design are presented.

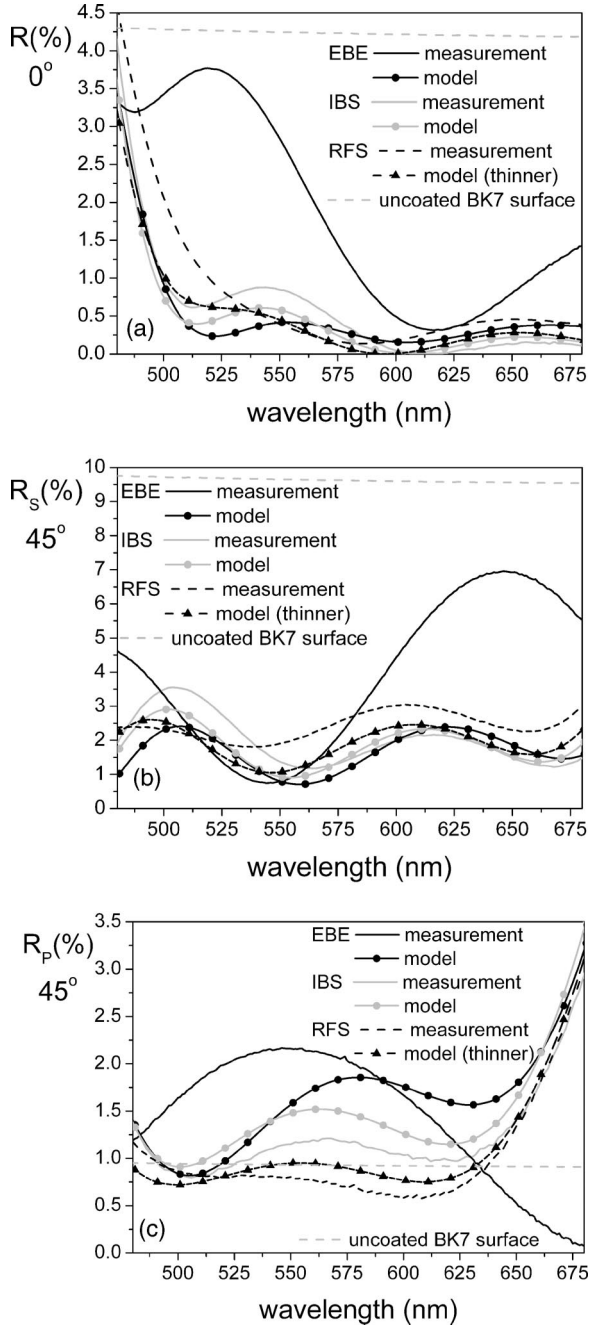

Fig. 4. Experimental and theoretical reflectance spectra of samples coated on both sides. Spectra of the thinner coatings and designs are shown at (a) 0°, (b) *s* and (c) *p* polarization at 45° angle of incidence. Reflectance of one uncoated glass surface is also shown for comparison. Note the higher discrepancy between the model and reflectance for EBE samples coated on both sides [most clearly seen in (a)] compared with the discrepancy for the EBE one-side coated sample [Fig. 3(a)] that originates from an accumulation of error (errors in second coating added to the errors in the first coating). (See also Fig. 5).

spectra directly on the rotating substrate. The corresponding spectra in a range from 475 to 950 nm were processed to continuously calculate the actual layer thicknesses and thus the layer termination points.

Selected deposition parameters for the fabricated hybrid antireflection samples are presented in Table 2. The coating was deposited on BK7 glass substrates on one side and on both sides, respectively. *Ex situ* transmittance and reflectance measurements were performed with a Perkin Elmer Lambda 900 spectrophotometer at 0°, as well as *s* and *p* polarizations at a 45° angle of incidence. An attachment allowing the absolute measurement of reflectance without moving the sample after the transmittance measurement was used.

D. Results and Discussion

Reflectance spectra of samples with hybrid AR coating deposited at one side and both sides of the substrate are presented in Figs. 3 and 4, respectively. The theoretical curves of the corresponding designs are also shown for comparison. A good matching of the theoretical and experimental curves for a 45° angle of incidence indicate also that the specification for a 50° angle of incidence ($R_s = R_p$) is well met. Samples with the thinner design (Fig. 1) are deposited with all three techniques. The quality of their performance can be compared by evaluating standard deviation values of the measured spectra from the theoretical data, defined in a similar way as in Eq. (1), except that the target values of reflectance are replaced by experimental values in the wavelength range 480–680 nm, measured in steps of 2 nm; the angles of incidence here are 0° and 45°. The calculated values of deviations for both sets of samples (one-side and both-side coated) are shown in Table 3. When comparing the results one has to keep in mind that the thicker coating, deposited by RFS, is more challenging for the production process than the thinner coatings, and, therefore, the probability of error is higher. Obviously, the IBS sample shows the lowest deviation from the theoretical spectrum. This quasi-inhomogeneous coating is the only one that corresponds, in fact, to the proposed design, where ramps are replaced by eight homogeneous refractive index layers. In this sense electron-beam evaporation (EBE) and RFS designs are only approximations for the cor-

Table 3. Comparison with Theory and Reproducibility[a]

Technique		$\delta_{1\,exp}$	$\delta_{2\,exp}$	$\delta_{1+1\,exp}$
EBE		0.107	0.253	0.047
RFS	Thinner	0.064	0.079	—
	Thicker	0.132	—	0.138
IBS		0.015	0.051	0.006

[a] $\delta_{1\,exp}$ stands for the deviation of the reflectance of the best one-side coated sample for a given technique from the corresponding theoretical reflectance of the model (presented in Fig. 3). $\delta_{2\,exp}$ denominates the corresponding parameter for samples coated on both sides (presented in Fig. 4). $\delta_{1+1\,exp}$ is the deviation between performances of two samples coated on one side but in different runs (presented in Fig. 5). $\delta_{1\,exp}$ and $\delta_{2\,exp}$ are calculated in the range 480–680 nm and $\delta_{1+1\,exp}$ in the range 400–950 nm. The high deviations of the RFS thicker samples may be attributed to spectral shifts (see Fig. 5) induced by the different thicknesses of the coatings.

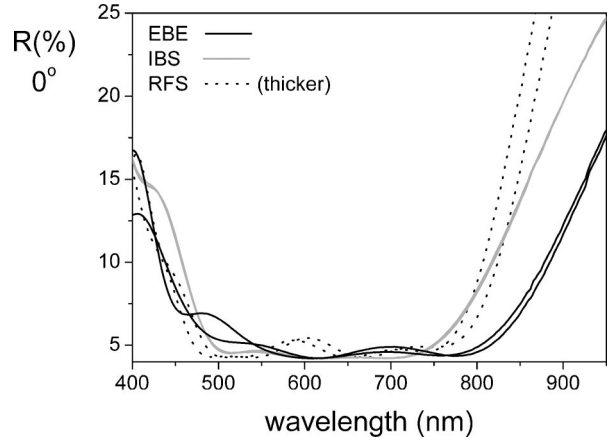

Fig. 5. Reproducibility of the results. Comparison of the spectra of two one-side coated samples produced with the same technique but in two different runs presented for each of the techniques.

responding coatings that have actually been deposited, where the changes in the refractive index are realized as linear ramps and not as step functions as in the designs. One could argue that this is the reason for the superior performance of IBS samples with respect to EBE and RFS samples. However, we have checked that a subdivision of the design ramps into 8 or 50 layers (this gives sublayers of approximately 2.5 nm of thickness and is without doubt a good approximation of linear ramps) gives a difference in theoretical performance that is too small to explain the weaker matching in performance of EBE and RFS designs and samples. Therefore we conclude that the quality of the IBS samples really originates from the high stability of the process and the reproducibility of the results in conjunction with the sophisticated *in situ* broadband monitoring and not from its quasi-inhomogeneous nature.

To check the reproducibility of the results for each technique, the reflectance spectra of the samples coated with the identical design, but made in different runs, were compared. They are represented in Fig. 5 and deviations of one from the other, δ_{1+1}, are shown in Table 3. Again, the IBS samples show much better reproducibility then the others. The high deviation of the RFS thicker sample, showing low reproducibility, may be attributed to spectral shifts (see Fig. 5) induced by the systematic error in the thickness of the coatings.

4. Conclusions

We have demonstrated successful coating processes for the fabrication of hybrid AR coatings. Samples coated by different techniques and experimental setups for deposition have been shown and the reproducibility of results compared. It has been shown that the samples with the best performances and reproducibility were obtained by IBS, demonstrating the high stability and reproducibility of this concept. Very good results were obtained by RFS as well. A sputtering technique with low rates of deposition permits a stable and precise deposition of mixture films. Omnidirectional AR coatings obtained by EBE, which allows for significantly higher deposition rates than the considered sputter processes, also show good optical performance.

There is still room for further improvement of the experimental setup for the EBE and the RFS processes, such as more precise calibration and control of rates of deposition. The deposition rates of the magnetron-sputtering process could be increased by at least 1 order of magnitude by using metallic targets and/or a different process setup (dynamic coating and midfrequency technique). The rates of the IBS process could also be increased by increasing the beam current.

Control of the deposition process by means of broadband optical monitoring[20,21] is especially helpful for online detection and compensation for deposition errors. *In situ* ellipsometry is a good tool for monitoring of optical properties and deposition rates as well, and has been used successfully for this purpose.[22] Due to measuring relative changes of intensities, this method is self-compensating and allows extremely precise measurements especially over longer deposition periods. *In situ* acquisition of spectra during the deposition can also help the optical characterization by detecting the origin of errors.

Although the EBE samples were, as expected, less successful due to more difficulties in control of the process because of high rates of deposition, it would be worth investing time and effort into improvements because this technique, having the highest rate of deposition, requires the least time for deposition of a coating and is the most commonly used technique. The potential for the homogeneous deposition of larger areas using the magnetron-sputtering process may in some situations compensate for the lower deposition rates compared with those for EBE.

The authors thank the German Federal Ministry of Economics and Labor (BMWA) for financial support within the research project Rugate Filters. V. Janicki thanks the Fraunhofer Society in Germany for a Fraunhofer Fellowship at the Institut für Angewandte Optik und Feinmechanik (IOF) in Jena. The authors thank Heidi Haase for technical assistance.

References

1. A. V. Tikhonravov, "Some theoretical aspects of thin-film optics and their applications," Appl. Opt. **32,** 5417–5426 (1993).
2. R. R. Willey, *Practical Design and Production of Thin Films* (Dekker, 2002) pp. 65–83.
3. J. A. Dobrowolski, D. Poitras, P. Ma, H. Vakil, and M. Acree, "Toward perfect antireflection coatings: numerical investigation," Appl. Opt. **41,** 3075–3083 (2002).
4. D. Poitras and J. A. Dobrowolski, "Toward perfect antireflection coatings. 2. Theory," Appl. Opt. **43,** 1286–1295 (2004).
5. E. Lorenzo, C. J. Oton, N. E. Capuj, M. Ghulinyan, D. Navarro-Urrios, Z. Gaburro, and L. Pavesi, "Porous silicon-based rugate filters," Appl. Opt. **44,** 5415–5421 (2005).
6. A. Kaless, U. Schulz, P. Munzert, and N. Kaiser, "NANOmotheye antireflection pattern by plasma treatment of polymers," Surf. Coat. Technol. **200,** 58–61 (2005).
7. I. M. Thomas, "Method for the preparation of porous silica antireflection coatings varying in refractive index from 1.22 to 1.44," Appl. Opt. **31,** 6145–6149 (1992).

8. P. Prene, J. J. Proittron, L. Beavrain, and P. Belleville, "Preparation of a sol–gel broadband antireflective and scratch resistant coating for blast shields of the French laser LIL," J. Sol-Gel Sci. Technol. **19,** 533–537 (2000).
9. H. Bartzsch, S. Lange, P. Frach, and K. Goedicke, "Graded refractive index layer system for antireflective coatings and rugate filters deposited by reactive pulse magnetron sputtering," Surf. Coat. Technol. **180–181,** 616–620 (2004).
10. M. F. Ouellette, R. V. Lang, K. L. Yan, R. W. Bertram, R. S. Owles, and D. Vincent, "Experimental studies of inhomogeneous coatings for optical applications," J. Vac. Sci. Technol. A **9,** 1188–1192 (1991).
11. V. Janicki, S. Wilbrandt, O. Stenzel, D. Gäbler, N. Kaiser, A. Tikhonravov, M. Trubetskov, and T. Amotchkina, "Hybrid optical coating design for omnidirectional antireflection purposes," J. Opt. A, Pure Appl. Opt. **7,** L9–L12 (2005).
12. V. Janicki, R. Leitel, S. Wilbrandt, O. Stenzel, D. Gäbler, and N. Kaiser, "Design of hybrid coatings composed of homogeneous layers and refractive index gradients," in *Advances in Optical Thin Films II,* C. Amra, N. Kaiser, and H. A. Macleod, eds., Proc. SPIE **5963,** 397–404 (2005).
13. A. V. Tikhonravov, M. K. Trubetskov, T. V. Amotchkina, M. A. Kokarev, N. Kaiser, O. Stenzel, S. Wilbrandt, and D. Gäbler, "New optimization algorithm for the synthesis of rugate optical coatings," Appl. Opt. **45,** 1515–1524 (2006).
14. Z. Knittl, *Optics of Thin Films* (Wiley, 1976) pp. 41–68.
15. R. Leitel, O. Stenzel, S. Wilbrandt, D. Gäbler, V. Janicki, and N. Kaiser, "Optical and nonoptical characterization of Nb_2O_5-SiO_2 compositional gradient index layer and rugate structures," Thin Solid Films **497,** 135–141 (2006).
16. O. Stenzel, S. Wilbrandt, D. Gäbler, N. Kaiser, A. V. Tikhonravov, M. K. Trubetskov, T. V. Amotchkina, and M. A. Kokarev, "Refractive indices of SiO_2 and Nb_2O_5 mixture films," in *Proceedings of VI International Conference "Prikladnaja Optika"* (Roshdestvensky Optical Society, 2004), vol. 3, pp. 34–38.
17. H. Ehlers, K. Becker, R. Beckmann, N. Beermann, U. Braunneck, P. Fuhrberg, D. Gäbler, S. Jakobs, N. Kaiser, M. Kennedy, F. König, S. Laux, J. C. Müller, B. Rau, W. Riggers, D. Ristau, D. Schäfer, and O. Stenzel, "Ion assisted deposition processes: industrial network IntIon," in *Advances in Optical Thin Films,* C. Amra, N. Kaiser, and H. A. Macleod, eds., Proc. SPIE **5250,** 646–655 (2004).
18. M. Lappschies, B. Görtz, D. Ristau, "Application of optical broad band monitoring to quasi-rugate filters by ion-beam sputtering," Appl. Opt. **45,** 1502–1506 (2006).
19. M. Lappschies, B. Görtz, and D. Ristau, "Optical monitoring of rugate filters," in *Advances in Optical Thin Films II,* C. Amra, N. Kaiser, and H. A. Macleod, eds., Proc. SPIE **5963,** 547–555 (2005).
20. K. Starke, T. Gross, M. Lappschies, and D. Ristau, "Rapid prototyping of optical thin film filters," in *Optical and Infrared Thin Films,* M. L. Fulton, ed., Proc. SPIE **4094,** 83–92 (2000).
21. S. Wilbrandt, N. Kaiser, and O. Stenzel, "*In situ* broadband monitoring of optical coatings," in *Proceedings of the Fifth ICCG* (Saarbruecken, 2004), pp. 429–433.
22. M. Vergöhl, N. Malkomes, T. Staedler, T. Matthée, and U. Richter, "*Ex situ* and *in situ* spectroscopic ellipsometry of MF- and DC-sputtered TiO_2 and SiO_2 films for process control," Thin Solid Films **351,** 42–47 (1999).